JOURNAL OF GUIDANCE, CONTROL, AND DYNAMICS
Vol. 16, No. 5, September–October 1993

Automatic Carrier Landing System Utilizing Aircraft Sensors

John L. Crassidis,* D. Joseph Mook,† and James M. McGrath*
State University of New York at Buffalo, Buffalo, New York 14260

A new closed-loop control system is developed and evaluated for use in automatic carrier landings. The system is based on a new tracking filter that uses angle of attack and airspeed measurements from the airplane, in addition to the usual ship-based radar measurements. The filter dynamic model is based on actual flight dynamics, using the additional measurements, and thus achieves significant radar noise sensitivity reduction by eliminating the existing dependence on numerical differentiation of the radar output. An additional feedback loop that blends aircraft model estimates with radar measurements is also added to the system. Nonlinear optimization techniques are used to determine a set of optimal filter and control gains for the entire closed-loop system. A detailed digital computer simulation, verified with available flight data, indicates that the use of the flight-dynamics-based tracking filter and the addition of the feedback loop dramatically improves the noise rejection sensitivity in the automatic carrier landing system.

Introduction

Background

AN automatic carrier landing system (ACLS) provides flight approach control until touchdown on an aircraft carrier.[1-3] The primary motivation for the use of the ACLS is low-visibility weather. Other concerns include atmospheric turbulence, deck motion caused by high seas, pilot fatigue at the end of difficult missions, etc.

The ACLS shipboard subsystems consist of a radar tracking system, a digital computer, and a transmitter. Aircraft subsystems include a pitch autopilot and an automatic thrust compensator (both described in detail in a later section). Under normal operating conditions, the small pitch and roll angles encountered during the landing approach enable the decoupling of the vertical (altitude) and horizontal (sideslip) control systems. Because of space limitations, the remainder of this paper is limited to vertical control, although the techniques used are easily extended to horizontal control.

Currently, ACLS vertical control proceeds as follows: First, the shipboard SPN-42 radar tracking system measures the aircraft's position with respect to the carrier. The shipboard computer uses this information to calculate a corrective pitch command. This command is then transmitted to the aircraft's autopilot and thrust compensator. The autopilot maintains the commanded pitch attitude, while the thrust compensator maintains a nominal angle of attack. By changing aircraft pitch while maintaining constant angle of attack, the inertial flight-path angle can be used to control changes in altitude.

Radar Noise

Sensor noise levels can create problems in the response characteristics of any feedback control system. Generally, if the feedback control gains are relatively high, then sensor noise produces a high noise content in the control signal. In the ACLS, high noise content in the pitch command results in a "bumpy" approach for the pilot. This can decrease the pilot's comfort and confidence in the control system's ability to safely land the aircraft, due to excessive control action, and is generally undesirable. But if the gains are lowered to reduce the noise levels in the pitch command, then closed-loop stability is adversely affected (due to increased response time). Therefore, a tradeoff between sensor noise reduction and system stability is required. Reference 3 contains detailed examples of these problems.

Previous simulation results[3] showed that the addition of a "noise rejection feedback loop" lowers the sensitivity of the pitch command to noise. However, this occurs at the expense of an increased turbulence response. Limiting the aircraft response to turbulence is a primary objective of the ACLS. Consequently, motivation exists for finding new methods to lower the noise content of the pitch command without simultaneously increasing the turbulence response of the aircraft.

The ACLS control law (described in a later section) uses estimates of the altitude and its first two derivatives to calculate the pitch command. However, the radar provides measurements of the altitude only, and these measurements generally contain some noise. An $\alpha - \beta$ tracking filter is currently used to produce the position and derivative estimates for the controller, using the radar measurements. The derivative estimates are obtained by numerical differentiation of the noisy altitude measurements, so that either 1) the noise content is amplified in the numerical derivatives or 2) the response speed is lowered due to the filtering.

In this paper, a new tracking filter is implemented for reducing the noise content of the altitude and derivative estimates, without reducing response speed. The approach is to replace the current $\alpha - \beta$ tracking filter with a flight-dynamics-based tracking filter. The dynamic filter uses airspeed and angle-of-attack measurements from the aircraft to create an "acceleration measurement," using a simplified lift model. Noise levels are greatly reduced by reducing or eliminating the need for numerical differentiation. Tracking accuracy is increased, producing a control signal containing significantly less noise than the existing system without sacrificing response speed or turbulence response. The step response characteristics are enhanced, whereas the turbulence response can be maintained to within original specifications.

Aircraft Model

Since operational ACLS flight information is available for an F-4 aircraft,[4] all computer simulation trajectories are produced with this aircraft. The aircraft simulation is a full approach simulation, derived using a 12th-order state-space model, representing the rigid-body aircraft dynamic equations of motion, and the concept of static stability using aircraft forces and moments (see any flight dynamics textbook, e.g., Nelson[5] or Roskam,[6] for details of the equations of motion).

Presented as Paper 91-2666 at the AIAA Guidance, Navigation, and Control Conference, New Orleans, LA, Aug. 12-14, 1991; received Dec. 26, 1991; revision received June 5, 1992; accepted for publication Nov. 21, 1992.

*Research Assistant, Department of Mechanical and Aerospace Engineering. Member AIAA.

†Associate Professor, Department of Mechanical and Aerospace Engineering. Senior Member AIAA.

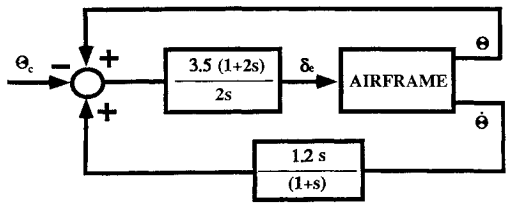

Fig. 1 Pitch attitude autopilot.

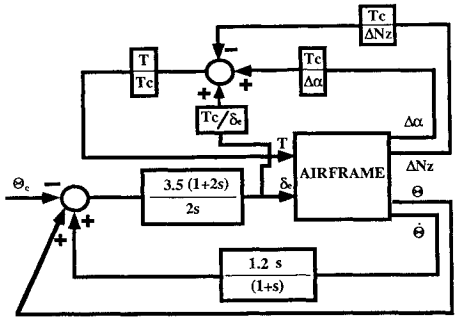

Fig. 2 Autopilot and thrust compensator.

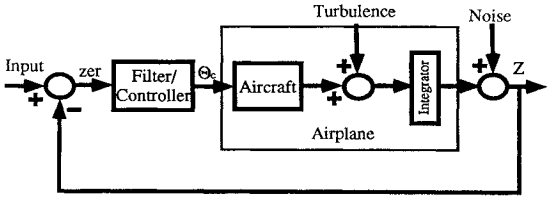

Fig. 3 Automatic carrier landing system block diagram.

Pitch Autopilot

The basic block diagram for the closed-loop system of the pitch autopilot with attitude feedback is shown in Fig. 1. A pitch command Θ_c is first introduced into the closed loop. A pitch angle error signal, representing the difference between the measured pitch angle Θ and the commanded pitch angle, is the input to the controller. The controller produces changes in the elevator setting δ_e, relative to a datum (typically, the trim value). The aircraft then responds to the new elevator setting with changes in pitch angle, pitch rate, vertical acceleration, and angle of attack.

Frequency domain techniques are used to evaluate the response characteristics of the attitude closed-loop system. The frequency domain pitch characteristics of an aircraft are characterized by the short period and phugoid modes. These transfer functions are derived by linearizing the nonlinear aircraft equations of motion.[7] Stability tests are possible by replacing the nonlinear aircraft model with the linear approximations. Results[5] show that closing the autopilot loop with just attitude feedback achieves the desired pitch angle. However, the system damping is decreased. To achieve significant damping and dynamic performance, a pitch rate $\dot{\Theta}$ feedback is also provided (Fig. 1).

Automatic Thrust Compensator

The autopilot achieves the commanded pitch angle, but it is the flight-path angle γ that must be controlled to land the aircraft using the ACLS. One method of achieving a commanded flight-path angle is to control the angle of attack to a desired reference point (e.g., the trim value) while controlling pitch, since the flight-path angle represents the difference between the pitch angle and angle of attack. This is accomplished by using the thrust compensator. The combined closed-loop system of the pitch autopilot coupled with the thrust compensator is shown in Fig. 2. The angle-of-attack error $\Delta\alpha$ signal (the difference between the measured value and the reference value) is sent to a controller, which develops command thrust changes for the aircraft. Changes in vertical acceleration ΔN_z are also controlled by a feedback loop, which helps to minimize the effects of turbulence.

Coupling of the Autopilot and Thrust Compensator

The thrust compensator does not respond to a pitch command but rather to a change in angle of attack or vertical acceleration. Response can be delayed for an indefinite period, based on the aircraft's response time. To create a faster response speed in the thrust compensator, an elevator feedback loop is used. This feedback loop leads the aircraft's response, so that the thrust compensator is engaged *before* a change in angle of attack or a change in vertical acceleration is detected. The feedback signals from the elevator, angle of attack, and vertical acceleration measurements are then summed and converted to a thrust command signal T_c. In the simulation, the thrust command is converted to the actual thrust change T by an engine lag transfer function $[T(s)/Tc(s)]$, and the loop is then closed by feeding back this thrust change to the aircraft model. Transfer functions for the remaining blocks in Fig. 2 can be found in Ref. 4. The autopilot and thrust compensator closed-loop operation continues until the commanded flight-path angle is achieved.

Verification from Experimental Trials

Simulation results show the aircraft response to step inputs for the pitch command (details of the simulation are given in Ref. 7). Frequency domain responses, in the form of Bode plots, show a close match to experimental data given by Bell Aerospace.[4] The autopilot and thrust compensator have a flight-path response bandwidth of about 1.4 rad/s, which is required to achieve good glide slope control. Using a root locus technique, the actual control gains[4] in the autopilot and thrust compensator were found to be accurate in the simulation.

Carrier Landing System

The block diagram for the current ACLS is shown in Fig. 3. An altitude command is first introduced into the closed loop. This command is used to calculate an error signal (*zer*) between the desired altitude and the measured altitude (obtained from radar). The error signal is then amplified and sent to an $\alpha - \beta$ filter,[4] which estimates the aircraft's vertical acceleration, velocity, and position errors. These estimates are denoted $\ddot{z}_e$, $\dot{z}_e$, and z_e, respectively. The filter estimates are then sent to a proportional-integral-derivative-double derivative (P-I-D-DD) controller,[4] which produces a corrective pitch command. This command signal is transmitted to the aircraft's pitch autopilot and thrust compensator. The response characteristics of the aircraft (altitude, angle of attack, airspeed, etc.) are determined by the pitch command.

To simulate the radar tracking system, a sinusoidal noise (4 rad/s) is added to the altitude response. This sinusoidal model is used because the radar measurement noise is dominated by electronic noise due to conical-scan modulations from radar pulse amplitudes.[8] Also, the frequency of 4 rad/s is the approximate corner frequency of the controller and produces the largest effects on the pitch command.

Controller

The block diagram for the P-I-D-DD controller is illustrated in Fig. 4. A discrete integrator equation is first derived by a numerical approximation:

$$\Theta_i(n) = \Theta_i(n-1) + \frac{V_g^2 K_P}{K_I}\left[\frac{z_e(n) + z_e(n-1)}{2}\right]\Delta t \qquad (1)$$

where V_g is a factored gain constant, K_P is the proportional gain, and K_I is the integral gain. The arguments n, $n-1$, etc., refer to discrete sampling times t_n, t_{n-1}, etc. A pitch command is then calculated using a P-I-D-DD control strategy along with the filtered error estimates as

$$\Theta_c'(n) = V_g K_P \left\{ z_e(n) + \left[K_D \dot{z}_e(n) + K_{DD} \ddot{z}_e(n) \right] \right\} + \Theta_i(n) \quad (2)$$

where K_D is the derivative control gain and K_{DD} is the double derivative gain.

To prevent too-rapid changes in the pitch command, it is low pass filtered before being transmitted to the airplane:

$$\Theta_c(n) = \Theta_c(n-1) + \alpha_p \left[\Theta_c'(n) - \Theta_c'(n-1) \right] \quad (3)$$

where α_p is the low-pass filter gain, and $\Theta_c(n)$ is the actual pitch command transmitted to the aircraft's pitch autopilot.

Current Tracking Filter

The position and velocity error estimates (z_e, $\dot{z}_e$), incorporated by the controller, are currently obtained using an $\alpha - \beta$ filter, summarized as

$$\begin{aligned} z_e^p(n) &= z_e(n-1) + \dot{z}_e(n-1)\Delta t \\ z_e(n) &= z_e^p(n) + \alpha[zer(n) - z_e^p(n)] \\ \dot{z}_e(n) &= \dot{z}_e(n-1) + \beta[zer(n) - z_e^p(n)]/\Delta t \end{aligned} \quad (4)$$

where $zer(n)$ is the difference between the desired altitude and the measured altitude. The filter gains (α and β) serve as weighting factors between the predicted error $z_e^p(n)$ and the measurement error $zer(n)$. These filter gains are bounded between 0 and 1.

The acceleration error estimate is obtained using the filtered error signal's second derivative:

$$\begin{aligned} \ddot{z}_e'(n) &= A_1[\ddot{z}_e'(n-1)] + A_2[\dot{z}_e(n) - \dot{z}_e(n-1)]/\Delta t \\ \ddot{z}_e(n) &= \ddot{z}_e'(n-1) + A_3[\ddot{z}_e'(n) - \ddot{z}_e'(n-1)] \end{aligned} \quad (5)$$

where $A_1 + A_2 = 1$. The special case where $A_2 = A_3$ is referred to as an $\alpha - \beta - \gamma$ filter (with $\gamma = A_2 = A_3$). Also, if α, β, A_1, A_2, and $A_3 = 1$, then the filter equations reduce to the normal back difference equations.

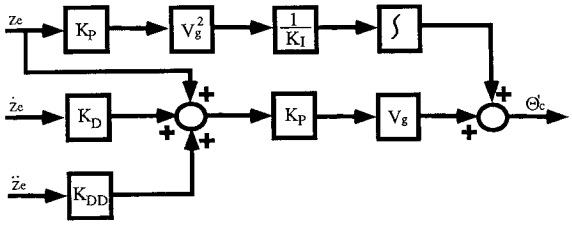

Fig. 4 P-I-D-DD controller.

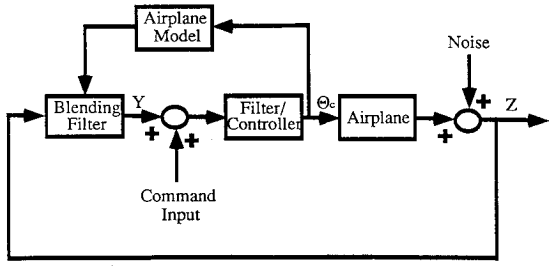

Fig. 5 ACLS with the noise rejection filter loop.

The $\alpha - \beta$ filter uses a finite difference for the prediction of the first and second derivatives of the measured error signal. Noise in the derivative estimates is amplified by opposite sign measurement errors in consecutive measurements. For example, if the noise has a positive sign in one measurement and a negative sign in the following measurement, then the derivative estimate is much lower than the actual derivative. If negative sign noise is followed by positive sign noise, the derivative estimate is much too high. This effect is even more pronounced in the second derivative.

Noise sensitivity is reduced when using small values for α and β, but this reduces the response to measured changes in altitude and thus reduces system response speed. In extreme cases, this can seriously affect closed-loop stability.

New Tracking Filter

Previous work has investigated the use of flight dynamics to construct tracking filters with force models (e.g., Refs. 9-12). Reference 13 summarizes these filters and develops a full force and moment model filter. The advantage of a force model is that it can be used to estimate acceleration, either instead of or in addition to numerical differentiation. Including force and moment models generally improves the tracking accuracy but imposes significantly higher computational burdens. McGrath[14] has investigated the tradeoffs between tracking accuracy and computational burden for the ACLS application. Considering altitude control, the dominant force is lift. Shyu[15] determined that 95% of the lift of the plane in landing approach can be modeled by

$$\text{lift} = (C_{L_0} + C_{L_\alpha}\alpha)\tfrac{1}{2}\rho \bar{V}^2 S \quad (6)$$

where C_{L_0} and C_{L_α} are aerodynamic coefficients, α is the angle of attack, S is related to wing geometry, ρ is air density, and $\bar{V}$ is airspeed. Measurements of the angle of attack and airspeed are therefore required to calculate the lift. Using the lift equation along with the vertical acceleration equation yields

$$\hat{\ddot{z}} = \frac{\text{lift} - \text{weight}}{\text{airplane mass}} \quad (7)$$

The flight-dynamics-based tracking is given as follows[14]:

$$\begin{aligned} \ddot{z}_e^p(n) &= \ddot{z}_e(n-1) \\ \ddot{z}_e(n) &= \ddot{z}_e^p(n) + G_1\left[\hat{\ddot{z}}(n) - \ddot{z}_e^p(n)\right] \\ \dot{z}_e^p(n) &= \dot{z}_e(n-1)\Delta t + \dot{z}_e(n-1) \\ z_e^p(n) &= 0.5\ddot{z}_e(n-1)\Delta t^2 + \dot{z}_e(n-1)\Delta t + z_e(n-1) \\ \dot{z}_e(n) &= \dot{z}_e^p(n) + G_2\left\{\left[zer(n) - z_e^p(n-1)\right]/\Delta t - \dot{z}_e^p(n)\right\} \\ z_e(n) &= z_e^p(n) + G_3\left[zer(n) - z_e^p(n)\right] \end{aligned} \quad (8)$$

where G_1, G_2, and G_3 are filter gains. To investigate the implementation of this filter in the ACLS, simulations of airspeed and angle-of-attack measurements are added to the closed-loop ACLS simulation. For simulation purposes, the measurement errors are assumed to be white Gaussian with $\sigma_\alpha = 0.5$ deg and $\sigma_s = 1.7$ ft/s.

Noise Rejection Feedback Loop

The flight-dynamics-based filter given by Eq. (8) is intended to reduce the noise content of the estimates $\ddot{z}_e$, $\dot{z}_e$, and z_e, which is expected to reduce the noise content in the pitch command. The noise rejection feedback loop reduces the noise content in the closed-loop pitch command regardless of the noise content in $\ddot{z}_e$, $\dot{z}_e$, and z_e. This is accomplished by sending an improved estimate of the error signal to the tracking filter (closed-loop block diagram is shown in Fig. 5). The blending

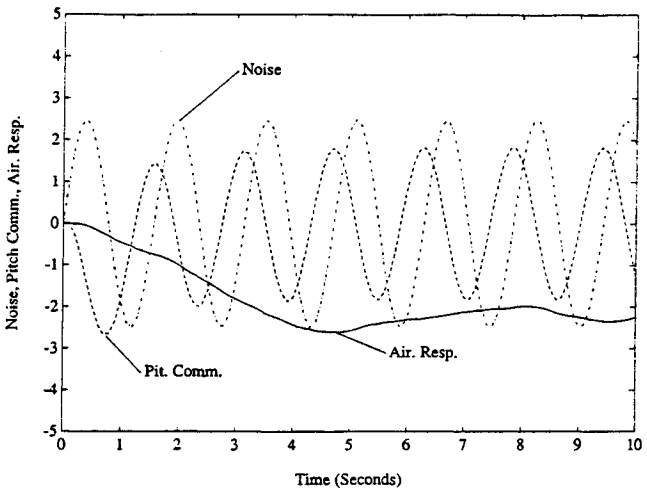

Fig. 6 Responses without the noise rejection loop.

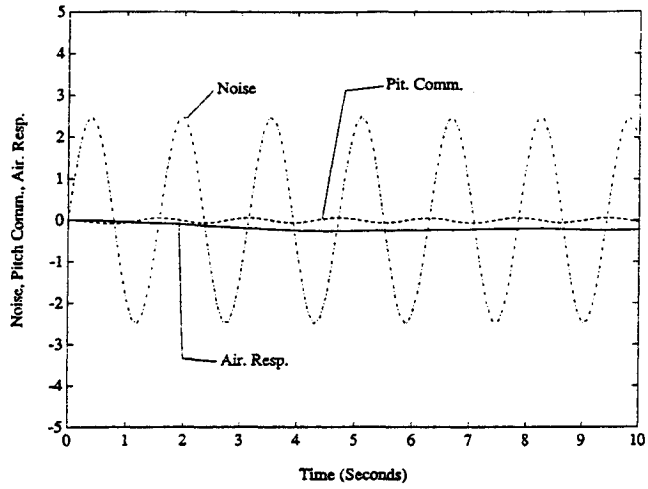

Fig. 7 Responses with the noise rejection loop.

filter portion of the feedback loop is represented by a Laplace domain transfer function:

$$Y(s) = \frac{Z(s) + A\hat{z}(s) + B\dot{\hat{z}}(s)}{1.0 + As + Bs^2} \tag{9}$$

where $Y(s)$ is the filter output, $Z(s)$ is the measured vertical position (from radar), $\hat{z}(s)$ is the velocity estimate, and $\dot{\hat{z}}(s)$ is the acceleration estimate from the aircraft model [Eq. (7)].

The parameters (A and B) are determined by optimizing the closed-loop system for noise rejection. Figures 6 and 7 illustrate the pitch command (degrees) and the aircraft's altitude response (feet) without and with the noise rejection loop, respectively. The simulation includes sinusoidal radar noise as previously described, and the command altitude is simply set to zero. The tracking filter is the currently used $\alpha - \beta$ filter. The ability of the noise rejection feedback loop to reduce noise in the pitch command and smooth the aircraft response is clearly shown. But, as shown in Ref. 3, this is at the expense of an increased turbulence response. This characteristic is unacceptable since turbulence response is a major concern during normal landing operations. Therefore, the problem of reducing noise sensitivity and simultaneously preventing an increase in turbulence response must be addressed (shown in a later section).

Experimental Turbulence

The random phenomenon of turbulence can only be described by statistical methods.[4] For a carrier landing, horizontal and vertical turbulence have a low cross correlation and can be separated to be analyzed individually.[6] The U.S. Navy and Bell Aerospace have performed various experiments to determine the magnitude and wavelength of the horizontal wind velocity.[4] Swanson[16] analyzed this data to determine changes in the aircraft's vertical velocity corresponding to horizontal turbulence. One data set (set 7.1) is shown in Fig. 8 (several data sets have been used in the simulation but are not shown).

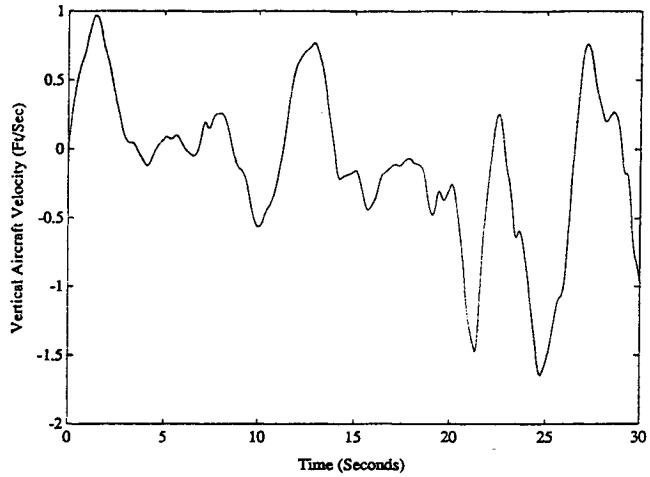

Fig. 8 Aircraft velocity change to turbulence.

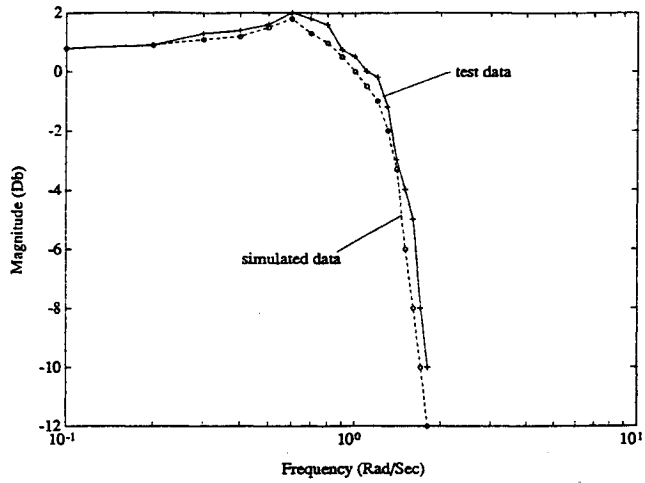

Fig. 9 Magnitude Bode plot comparison.

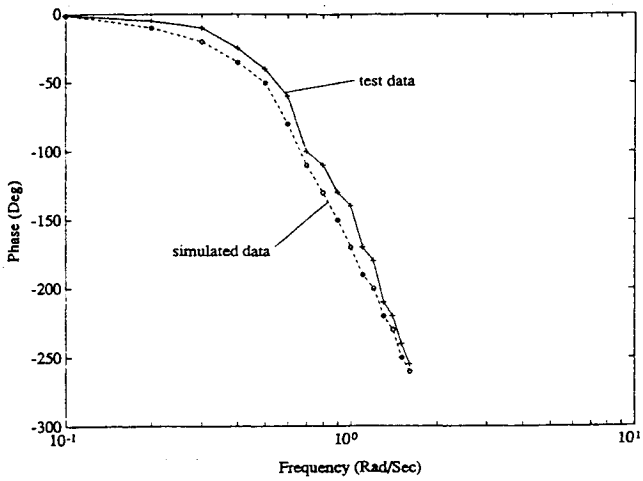

Fig. 10 Phase Bode plot comparison.

Frequency Response

Experimental Bode plot data (altitude response to an altitude command) for the current ACLS without the noise rejection feedback loop (NRFL) is provided by Bell Aerospace.[4] This is compared with the computer simulation Bode data as shown in Figs. 9 and 10 (the solid line is experimental data).

The magnitude and phase Bode plot results indicate that the simulated response characteristics closely match the experimental data. Also, the Bode plot shows a response bandwidth of approximately 1.4 rad/s. These results are similar to the Urnes and Hess[1] results for an F/A-18 aircraft in an ACLS operation.

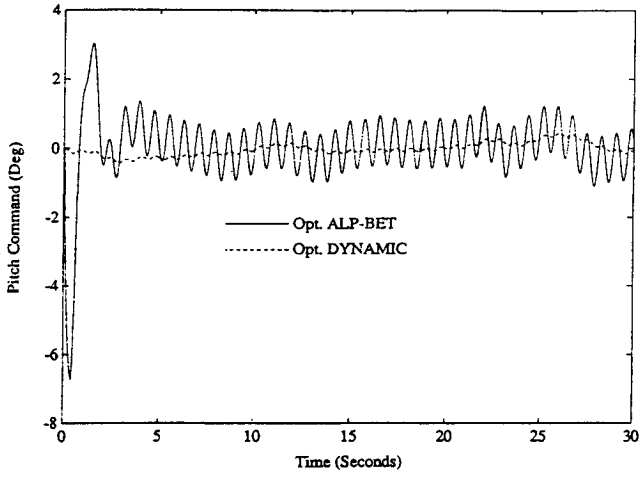

Fig. 11 Optimized pitch command (without NRFL).

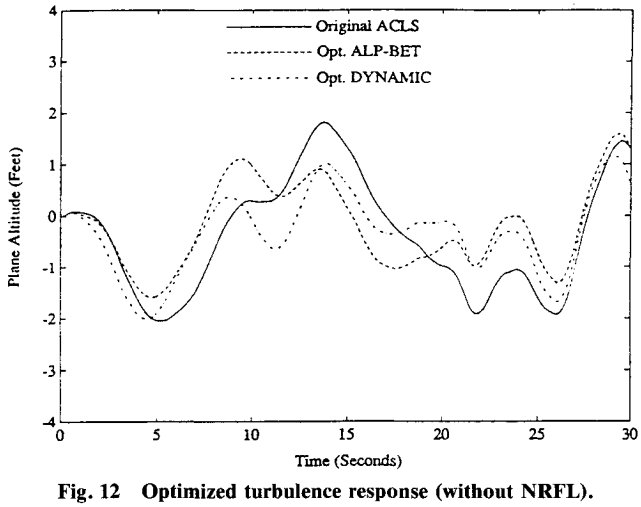

Fig. 12 Optimized turbulence response (without NRFL).

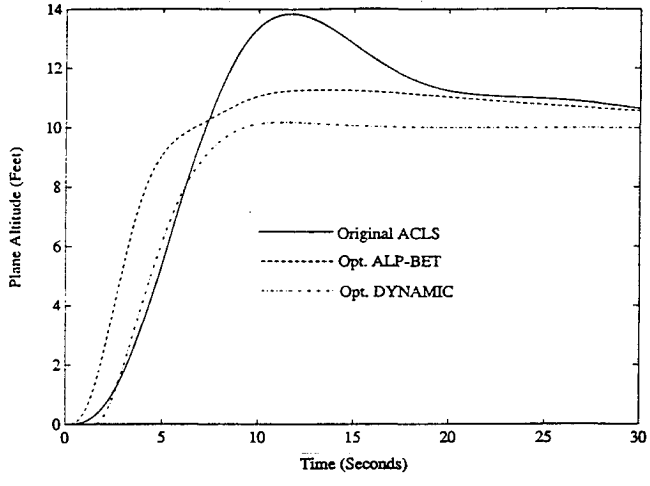

Fig. 13 Optimized step response (without NRFL).

Table 1 Comparison of step responses

	Original ACLS gains	Optimized $\alpha-\beta$ filter	Optimized dynamic filter
Overshoot, %	45	20	3
Rise time, s	3	4	5
Settling time, s	25	28	18

Table 2 Comparison of individual cost functions

	Original ACLS gains	Optimized $\alpha-\beta$ filter	Optimized dynamic filter
Noise, ave.	362,285	148,195	14,971
Turbulence, ave.	1,094	1,102	1,085
Step response	1,429	1,232	1,056
Total cost	364,808	150,529	17,112

Table 3 Comparison of rms values for turbulence

Data set	Original ACLS gains	Optimized $\alpha-\beta$ filter	Optimized dynamic filter
7.1	1.94	2.01	1.96
7.3	2.47	2.50	2.43
7.6	2.55	2.61	2.51

Variable Optimization

To develop a comparison study between the $\alpha-\beta$ tracking filter and the flight-dynamics-based tracking filter, a control/filter variable optimization is performed. This scheme minimizes a cost function of the errors in the aircraft response, treating the control and filter gains as the variables of optimization.

Four cases for the optimization are performed. The ACLS using the current $\alpha-\beta$ tracking filter and the ACLS using the flight-dynamics-based tracking filter are each optimized with and without the NRFL. Therefore, an optimum tracking filter choice can be determined.

Since the optimization is numerically defined, several methods are used to insure that a global minimum is located. These techniques include exterior and interior penalty functions, steepest descent, conjugate gradient, and conjugate directions (e.g., Ref. 17).

The variables in the optimization include α, β, A_1, A_2, and A_3 for the current tracking filter; G_1, G_2, and G_3 for the flight-dynamics-based tracking filter; the gains K_P, K_I, K_D, and K_{DD} from the controller; and the gains A and B for the noise rejection feedback loop.

Cost Function Analysis

The performance criterion for the optimization is evaluated with respect to an optimal noise rejection, filter tracking performance, turbulence response, and step response. The combination of these criteria describes the optimal closed-loop performance.

The cost function is based on the integral of the error signal. A quadratic form, called the integral-squared-error (ISE), is used to insure a "well-defined" minimum.

The cost function used to reduce the noise levels in the pitch command is

$$\Phi_n = \int_{t_0}^{t_f} \left[W_1 \Theta_c^2(t) + W_2 \ddot{\Theta}_c^2(t) \right] dt \tag{10}$$

where W_1 and W_2 are weighting factors that reflect the relative importance between maintaining an adequate control signal Θ_c and eliminating high-frequency components $\ddot{\Theta}_c$ in the pitch command.

The turbulence response cost function minimizes the error between the desired altitude and the actual altitude. The commanded altitude for the turbulence response is zero, and the cost function is defined as

$$\Phi_t = \int_{t_0}^{t_f} \left[W_3 zer^2(t) \right] dt \tag{11}$$

The step response is used to analyze the aircraft's response to a step input signal. Step response is a good measure of response speed and stability. The step cost function is defined as

$$\Phi_s = \int_{t_0}^{t_f} \left[W_4 zer^2(t) + W_5 \ddot{\Theta}_c^2(t) \right] dt \tag{12}$$

The second term $\ddot{\Theta}_c$ insures adequate damping in the step response.

The tracking accuracy is optimized by minimizing the position, velocity, and acceleration estimate errors produced by the tracking filters. The tracking cost function is defined as

$$\Phi_f = \int_{t_0}^{t_f} \left[W_6 z_e^2(t) + W_7 \dot{z}_e^2(t) + W_8 \ddot{z}_e^2(t) \right] dt \tag{13}$$

Optimization of any one cost function produces an optimal response for that characteristic but a degradation of the other characteristics (e.g., optimizing for turbulence only degrades the step response). Therefore, a combined cost function is used. The objective is a small turbulence response, good noise rejection, high filter tracking accuracy, and optimal step response. The combined cost function is defined as

$$\Phi_c = W_9 \Phi_t + W_{10} \Phi_n + W_{11} \Phi_s + W_{12} \Phi_f \tag{14}$$

Selection of the weights W_1–W_{12} can be varied to trade off individual response characteristics of the overall system response. These weighting factors are selected to achieve high noise rejection capabilities, while maintaining or improving the step and turbulence response characteristics. Also, these weighting factors remain constant for each optimization case study. Therefore, a qualitative comparison of individual cost functions is possible.

Optimization Results (Without Noise Rejection Loop)

The optimized pitch command responses are shown in Fig. 11 (the solid line is the ACLS with the $\alpha - \beta$ filter, and the dashed line is with the flight-dynamics-based tracking filter). The optimized turbulence and step responses are shown in Figs. 12 and 13, respectively.

A comparison study of the original $\alpha - \beta$ filter/controller gains and optimized flight-dynamics-based filter/controller gains is made in tabular form. Tables 1–3 show the step response characteristics, cost function results, and rms values for various turbulence responses, respectively.

The combined cost function results clearly show an improvement in noise rejection and step response when using the flight-dynamics-based tracking filter, while maintaining an adequate turbulence response.

Optimization Results (with Noise Rejection Loop)

From Figs. 6 and 7, the use of the NRFL significantly reduces the sensor noise content in the pitch command. But the NRFL causes the aircraft to exhibit greater motion when subjected to turbulence as compared with the original ACLS response. Therefore, for the tracking filter/controller optimization with the NRFL, emphasis is placed on reducing the turbulence response.

The optimized pitch command response with the NRFL is shown in Fig. 14 (the solid line is the ACLS with the $\alpha - \beta$ filter, and the dashed line is with the flight-dynamics-based tracking filter). The optimized turbulence and step responses are shown in Figs. 15 and 16, respectively.

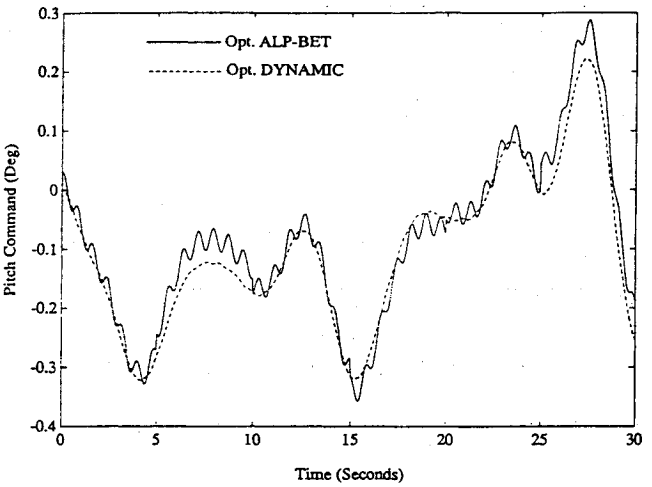

Fig. 14 Optimized pitch command (with NRFL).

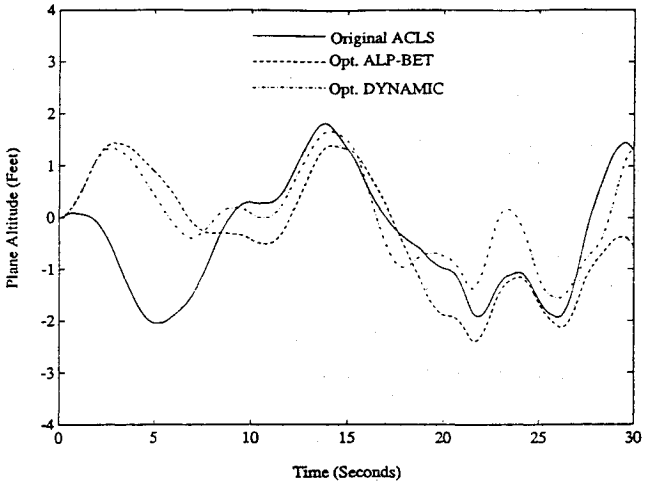

Fig. 15 Optimized turbulence command (with NRFL).

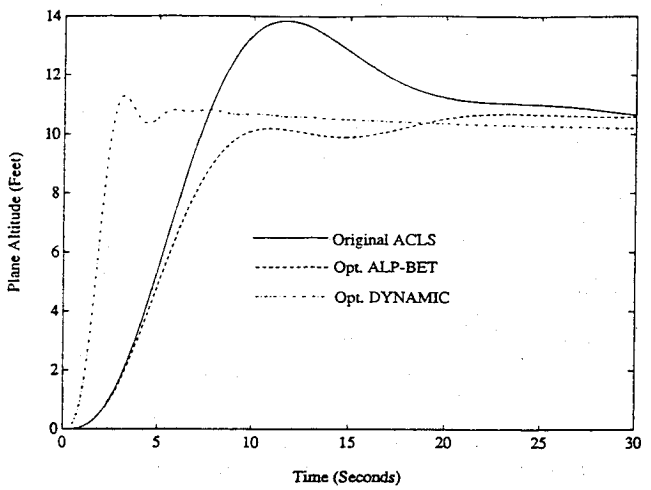

Fig. 16 Optimized step response (with NRFL).

From Fig. 14, the pitch command for the dynamic filter rejects nearly 100% of the noise content. Also, from Fig. 15, the turbulence response is minimized slightly *below* the original ACLS turbulence response (without the NRFL). Finally, the step response for the dynamic filter case shows a definite improvement as compared with the optimized $\alpha - \beta$ filter case. This is due to an accurate filter estimate for the acceleration error in the dynamic filter. Therefore, the double derivative control gain invokes a better step response for the dynamic filter.

Table 4 Comparison of step responses

	Original ACLS with NRFL	Optimized $\alpha-\beta$ filter	Optimized dynamic filter
Overshoot, %	45	12	11
Rise time, s	3	4.2	1.0
Settling time, s	25	26	15

Table 5 Comparison of individual cost functions

	Original ACLS with NRFL	Optimized $\alpha-\beta$ filter	Optimized dynamic filter
Noise, ave.	1676	1102	57
Turbulence, ave.	1276	1043	850
Step response	1429	896	556
Total cost	4831	3041	1463

Table 6 Comparison of rms values for turbulence

Data set	Original ACLS with NRFL	Optimized $\alpha-\beta$ filter	Optimized dynamic filter
7.1	2.32	2.12	1.86
7.3	2.80	2.51	1.91
7.6	2.94	2.73	2.36

Table 7 Effect of weight variation on the open-loop cost function

Weight, lb	Cost function	Percent change
+10%	2869	2.2
+5%	2899	1.16
0% = 32,414	2933	0
−5%	2977	1.49
−10%	3029	3.26

Tables 4–6 show the step function results, cost function results, and rms values for the turbulence response. The combined cost function results with the noise rejection loop clearly show a vast improvement in noise rejection, a slight improvement in turbulence response, and a moderate improvement in step response by incorporating the flight-dynamics-based tracking filter. Also, the optimized configuration maintains the rate-limited control actuators to within specified tolerances (e.g., the stabilator rate is within the 25-deg/s limit for the F-4). Therefore, the optimized gain configuration is realizable for use on the actual ACLS.

Effect of Flight Parameter Variation

The purpose of this section is to investigate how changing certain parameters in the F-4 model simulation affects the tracking results on the flight-dynamics-based tracking filter. The analysis includes an evaluation of performance sensitivities to realistic errors in the assumed values for weight, airspeed, angle of attack, and air density. This analysis is performed in an open-loop tracking filter response to a turbulence input. Therefore, the robustness of the new tracking filter is tested.

The procedure is to select a parameter (such as aircraft weight) and vary it by $\pm 10\%$. Other parameters, such as airspeed, angle of attack, etc., are then adjusted to restore an equilibrium flight path to the simulation (in the absence of a disturbance). The flight dynamics filter is then loaded with the previously optimized gains (open loop) with noisy measurements. The cost function is recorded and compared with the originally optimized cost function ($\phi = 2933$). The percent change indicates the sensitivity of the optimized gains to changes in the flight parameters.

The first analysis varies the aircraft weight by $\pm 10\%$, whereas the air density and airspeed are held constant. To achieve an equilibrium flight path (before the turbulence disturbance), the angle of attack, elevator, and thrust are adjusted. Table 7 shows the results of the weight variation.

The difference between cost functions does not exceed 3.26% for a 10% change in weight. The increase in cost function with decrease in weight may be due to the aircraft having less inertia and responding more quickly to a disturbance, and thus it is more difficult to track.

Similar results are obtained for variations in airspeed, angle of attack, and air density. The difference between cost functions does not exceed 3.2% for a 10% change in airspeed. The difference between cost functions does not exceed 1.16% for a 10% change in angle of attack. The difference between cost functions does not exceed 2.17% for a 10% change in airspeed. Also, 10% variations in aerodynamic coefficients (C_{L_0} and C_{L_α}) lead to a difference in cost functions not exceeding 4.2%. Therefore, the flight-dynamics-based filter's ability to track the vertical states is largely unaffected by changes of $\pm 10\%$ in a particular flight condition or setting.

Conclusions

In this paper, a new technique for decreasing a feedback control system's sensitivity to sensor noise while increasing system response characteristics is developed. This technique was applied to a flight-data-verified simulation of an autopilot/thrust compensator in conjunction with an automatic carrier landing system. A flight-dynamics-based tracking filter and a noise rejection feedback loop have been studied in the closed-loop simulation.

Nonlinear optimization techniques were used to determine the optimal performance of the current carrier landing system as compared with the landing system with the flight-dynamics-based tracking filter. A combined cost function related to noise rejection, turbulence response, and the step response was optimized to determine control and filter gains. Two optimization cases were performed. The first case involves the carrier landing system without the noise rejection feedback loop. The dynamic tracking filter outperformed the $\alpha-\beta$ tracking filter in the closed-loop response (noise rejection being the greatest improvement). The second case involves the carrier landing system with the noise rejection feedback loop. This feedback loop provides excellent noise rejection capabilities, but at the expense of an increased turbulence response. The optimized $\alpha-\beta$ tracking filter produced an adequate noise rejection, while preserving the original turbulence response. But the dynamic tracking filter rejected nearly 100% of the noise content in the pitch command. Also, the step response was improved and the turbulence response was slightly decreased from the original carrier landing system's response.

References

[1]Urnes, J. M., and Hess, R. K., "Development of the F/A-18A Automatic Carrier Landing System," *Journal of Guidance, Control, and Dynamics*, Vol. 8, No. 3, 1985, pp. 289–295.

[2]Urnes, J. M., Hess, R. K., Moomaw, R. F., and Huff, R. W., "H-Dot Automatic Carrier Landing System for Approach Control in Turbulence," *Journal of Guidance and Control*, Vol. 4, No. 2, 1981, pp. 177–183.

[3]Mook, D. J., Swanson, D. A., and Roemer, M. J., "Improved Noise Rejection in Automatic Carrier Landing Systems," *Journal of Guidance, Control, and Dynamics*, Vol. 15, No. 2, 1992, pp. 509–519.

[4]"Automatic Carrier Landing Compatibility," Bell Aerospace, Final Rept. 60003-180, Buffalo, NY, Feb. 1969.

[5]Nelson, R. C., *Flight Stability and Automatic Control*, McGraw-Hill, New York, 1987.

[6]Roskam, R. C., *Airplane Flight Dynamics and Automatic Control, Part 1 and 2*, Roskam Aviation and Engineering Corp., Univ. of Kansas, Lawrence, KS, 1979.

[7]Crassidis, J. L., and Mook, D. J., "Modeling an Autopilot and Thrust Compensator in an Automatic Carrier Landing System," *Pro-*

ceedings of the AIAA Flight Simulation Technologies Conference (New Orleans, LA), AIAA, Washington, DC, 1991 (AIAA Paper 91-2956).

[8]Biernson, G., *Optimal Radar Tracking Systems*, Wiley, New York, 1989.

[9]Singer, R. A., "Estimating Optimal Tracking Filter Performance for Maneuvering Targets," *IEEE Transactions on Aerospace and Electronic Systems*, Vol. AES-6, No. 4, 1970, pp. 473–483.

[10]Fitzgerald, R. J., "Simple Tracking Filters: Closed Form Solutions," *IEEE Transactions on Aerospace and Electronic Systems*, Vol. AES-17, No. 6, Nov. 1981, pp. 781–785.

[11]Kendrick, J. D., Maybeck, P. S., and Reid, J. G., "Estimation of Aircraft Target Motion Using Orientation Measurements," *IEEE Transactions on Aerospace and Electronic Systems*, Vol. AES-17, No. 2, 1981, pp. 254–259.

[12]Andrisani, D., Kuhl, F. P., and Gleason, D., "A Nonlinear Tracker Using Attitude Measurements," *IEEE Transactions on Aerospace and Electronic Systems*, Vol. AES-22, No. 5, 1986, pp. 533–539.

[13]Mook, D. J., Shyu, I. M., and Coye, K. B., "A Nonlinear Aircraft Tracking Filter Utilizing Control Variable Estimation," *Journal of Guidance, Control, and Dynamics*, Vol. 15, No. 1, 1992, pp. 228–238.

[14]McGrath, J., "Improved Aircraft Vertical State Tracking by Use of Flight Dynamics-Based, Kalman Filtering," Master's Thesis, Dept. of Mechanical Engineering, State Univ. of New York at Buffalo, Buffalo, NY, 1991.

[15]Shyu, I. M., "Enhanced Tracking of an Aircraft Utilizing Nonlinear Force, Moment and Control Estimation," Master's Thesis, Dept. of Mechanical Engineering, State Univ. of New York at Buffalo, Buffalo, NY, 1988.

[16]Swanson, D. J., "Optimization of Control and Filter Gains in an Automatic Carrier Landing System," Master's Thesis, Dept. of Mechanical Engineering, State Univ. of New York at Buffalo, Buffalo, NY, 1990.

[17]Reklaitis, G. V., Ravindran, A., and Ragsdell, K. M., *Engineering Optimization, Methods and Applications*, Wiley, New York, 1983.